Research Article
Open Access

Preparation of sodium alginate films incorporated with hydroalcoholic extract of *Macrocystis pyrifera* L.

**Judith Ramos[1], Nelson Adrián Villacrés[1],
Éder Tadeu Gomes Cavalheiro[2], Hugo A. Alarcón[1], Ana C. Valderrama[1],***

[1] National University of Engineering**ROR**, Lima, Peru
[2] University of São Paulo**ROR**, São Paulo, Brazil

* e-mail: ana.valderrama.n@uni.edu.pe

Abstract:
Agroindustry needs novel materials to replace synthetic plastics. This article introduces sodium alginate films with antioxidant properties. The films, which were incorporated with hydroalcoholic extract of *Macrocystis pyrifera* L., were tested on sliced Hass avocados.
The research featured sodium alginate films incorporated with hydroalcoholic extracts of *M. pyrifera*. Uncoated avocado halves served as control, while the experimental samples were covered with polymer film with or without hydroalcoholic extract. A set of experiments made it possible to evaluate the effect of the extracts on polymeric matrices, release kinetics, and sensory profile of halved Hass avocados.
A greater concentration of hydroalcoholic extracts increased the content of phenolic compounds and their antioxidant activity. As a result, the bands in the carboxylate groups of sodium alginate became more intense. Crystallinity decreased, whereas opacity and mass loss percentage increased, and conglomerates appeared on the surface of the films. These processes fit the Korsmeyer-Peppas kinetic model because they resulted from a combination of diffusion and swelling mechanisms in the films.
The films incorporated with hydroalcoholic extract of *M. pyrifera* proved to be an effective alternative to traditional fruit wrapping materials.
Keywords: Sodium alginate, films, hydroalcoholic extracts, *Macrocystis pyrifera*, coating, storage, avocado

INTRODUCTION

Polymers, popularly known as plastics, are usually synthetic or semi-synthetic organic compounds with a high molecular weight. These materials are used in almost all industrial sectors. As a result, the total amount of plastics manufactured in the world since 1950 exceeds 8000 Mt [1]. However, its production generates pollutants and greenhouse gases, e.g., carbon dioxide (CO_2), which contribute to environmental pollution and global warming [2].

However, conventional polymers can be replaced by biodegradable materials made of fats, vegetable oils, gluten, proteins, and polysaccharides [3].

Bioplastics are defined as materials produced by living organisms. They are biobased, biodegradable, or both and are used in many sectors, including food processing, agriculture, compost bags, etc. [4].

Red (*Rhodophyta*), green (*Chlorophyta*), and brown (*Phaeophyta*) macroalgae possess a great chemical diversity of primary and secondary metabolites with numerous beneficial properties and a good application potential. They have increasingly attracted attention of many industrial branches, including plastics production [5].

Brown macroalgae contain secondary metabolites with antioxidant, anti-inflammatory, and anti-

microbial [6, 7] properties. *Macrocystis pyrifera* is one of the most popular representatives of this group [8].

M. pyrifera L. is a low-calorie product with a high concentration of mineral ions (Mg^{2+}, Ca^{2+}, P^{5+}, K$^+$, I$^-$), vitamins, low lipid content, alginates, and polyphenols [9].

Polyphenols are antioxidant compounds that delay or prevent the oxidation of oxidizable molecules [10]. As a result, they reduce food deterioration when they are incorporated directly into food itself or its packaging [11].

Alginate is a polysaccharide that consists of *β*-D-mannuronic and *α*-L-guluronic acids [12]. It is biocompatible, biodegradable, low-toxic, and easily available, which causes a great commercial interest [13]. Alginate-based films and coatings are flexible and glossy; they possess excellent water solubility and emulsification capacity, as well as low oil and oxygen permeability [14].

In the food industry, alginate-based films provide temporary protection against water loss. Such films prolong the shelf life of fruits and vegetables by inhibiting post-harvest metabolic processes, i.e., aging and rotting [15]. Alginate-based films are prospective vehicles for polyphenolic compounds, which migrate, partially or totally, from the film onto the food surface [16, 17].

The extract leaves the polymeric matrix by diffusion throughout or swelling of the matrix. Eventually, the release rate decreases because the material swells, and the active agent has to cover a greater distance to exit the system. This diffusion process is governed by Fick's law, in which the concentration is proportional to the diffusion flux density.

However, some swelling-produced systems generate a slow migration, which results in a balance between the internal and external environments. Considering these processes, Higuchi proposed that release occurs as a function of the square root of time (Eq. (1)), while Korsmeyer *et al.* considered that the release depends on material dissolution or structural effects (Eq. (2)) [18, 19]:

$$\frac{M_t}{M_\infty} = K \times t^{1/2} \tag{1}$$

where M_t/M_∞ is the fraction of solute that has been released at time *t*, and *K* is the release rate constant;

$$\frac{M_t}{M_\infty} = K \times t^n \tag{2}$$

where *K* is a constant that incorporates structural and geometric characteristics of the release system, and *n* is the exponent that indicates the release mechanism.

This research focused on the antioxidant effect of sodium alginate films with hydroalcoholic extract of *M. pyrifera* on Hass avocado.

STUDY OBJECTS AND METHODS

Materials. All solvents and reagents were of analytical grade. Medium viscosity brown algae sodium alginate, glycerol 99%, average weight poly (ethylene) glycol Mn 400, sodium carbonate, the Folin-Ciocalteu reagent 2N, gallic acid, and 1,1-diphenyl-2-picrylhydrazyl (DPPH) were purchased from Sigma-Aldrich. Ethanol and methanol were produced by Merck. The hydroalcoholic extract of brown macroalgae was prepared from *Macrocystis pyrifera* L., collected in the district of Paracas (Ica, Peru). The Hass avocado fruits were collected from the Province of Chincha (Ica, Peru) and stored at 8°C until the application of the films.

Extraction of brown macroalgae with a hydroalcoholic solution. To produce the extracts, we macerated 10 g of dry and ground brown macroalgae with 100 mL of a hydroalcoholic ethanol:water solution (70:30, v/v). The mix was stirred at 35°C in an amber bottle for 24 h. Then, the mix was filtered, and the solid residue was macerated again with the hydroalcoholic solution. The resulting supernatants were combined and concentrated with a vacuum evaporator to a volume of 100 mL. The resulting product was stored at 10°C.

Determination of the total phenolic content. The total phenolic content of the hydroalcoholic extract was revealed by the Folin-Ciocalteu method, and the results were expressed in gallic acid equivalent per 100 g of brown macroalgae (mg GAE 100 g^{-1}) [20]. According to the standard procedure, 1 mL of the hydroalcoholic *M. pyrifera* extract was mixed with 0.6 mL of the Folin-Ciocalteu reagent. After that, we added 3.2 mL of an aqueous solution of sodium carbonate (Na$_2$CO$_3$, 7.5%, w/v). The resulting mix was brought up to 12 mL with ultrapure water and stirred at room temperature in the dark for 60 min. Finally, its absorbance was measured at 765 nm using a Lambda 25 UV-Vis spectrophotometer (Perkin Elmer).

Determination of the free radical capture capacity (DPPH method). *Antioxidant activity.* The antioxidant activity was determined using the 1,1-diphenyl-2-picrylhydrazyl (DPPH) method [21]. According to the standard procedure, 1 mL of the hydroalcoholic *M. pyrifera* extract was mixed with 1 mL of methanolic solution of DPPH (0.36 mmol L^{-1}) and 2 mL of methanol. The mix was stirred and left at room temperature in the dark for 30 min. Then, its absorbance was measured at 517 nm.

The results were expressed as the inhibition percentage of the DPPH radical according to Eq. (3):

$$\text{Inhibition}\,(\%) = 100 \times \left(\frac{A_C - A_E}{A_C} \right) \tag{3}$$

where A_C is the control absorbance (DPPH), and A_E is the extract absorbance.

Preparation of the films incorporated with hydroalcoholic extract. We added a mix of plasticizers (ethylene glycol and polyethylene glycol) to 30 mL of sodium alginate polymeric solution 1.5% (w/v) at

a ratio of 9:1 (w/w) under constant stirring at 70°C for 60 min. Subsequently, we added 5 mL of extract solution in a range between 3 and 6 % (w/v). The solution was obtained from the stock solution of *M. pyrifera* extract. The resulting mix was stirred at 70°C for 30 min. Finally, the solutions were molded and dried at 50°C for 24 h.

Description of the films incorporated with hydroalcoholic extract. The opacity was reduced from the transmission values and the film thickness as in Eq. (4). The mean thickness value was registered using a mechanical micrometer (Mitutoyo 103-137) with a precision of 0.01 mm. The transmittance value was obtained by cutting the films into square pieces (20×20 mm). The pieces were placed in the support of solid samples of a Varian Cary® 50 UV-Vis spectrophotometer. The spectra were registered at 300–1000 nm [22].

$$Opacity = \frac{-Log(T)}{d} \qquad (4)$$

where *T* is the light transmittance of the film at 600 nm, and *d* is the sample thickness, mm.

The FTIR spectra were obtained by Attenuated Total Reflectance (ATR) using an IRPrestige 21 Shimadzu spectrophotometer at 600–4000 cm⁻¹ after acquisition of 20 scans at a resolution of 4 cm⁻¹ for each spectrum. Thermogravimetric curves were gathered in an SDT Q600 simultaneous TG/DTA modulus managed by the Thermal Advantage for Q Series software (v. 5.5.24), both from TA Instruments.

The measurements were performed using sample amounts of 5.0 ± 0.1 mg in a dynamic N_2 atmosphere flowing at 50 mL min⁻¹. The temperature range was selected as 25–800°C with a heating rate of 10°C min⁻¹. The XRD diffractograms were obtained in a range of 2θ from 5 to 100° in a D8 Advance diffractometer (Brüker) equipped with a Cu source ($K\alpha = 1.5418$ Å) and a LynxEye model PSD type detector. The diffractometer operated at a voltage of 40 kV and 40 mA (1600 W). The SEM images were obtained with an LEO 440 microscope (Cambridge) equipped with a 7060 detector (Oxford) at resolutions of 10 and 1 μm with a magnification of 1000× and 5000×, respectively.

Table 1 Antioxidant activity of *Macrocystis pyrifera* extract at different concentrations

Extract %, w/v	Total phenolic content, mg GAE 100 g⁻¹	DPPH radical scavenging, %
3.0	25.4 ± 0.2	22.2 ± 0.2
6.0	48.5 ± 0.3	41.2 ± 0.4
10	74.2 ± 0.3	61.0 ± 0.1

The samples were gold-plated in an MED 020 (Bal-Tec) high vacuum metallizer.

Release test of hydroalcoholic extract. The alginate films incorporated with hydroalcoholic extract of *M. pyrifera* were immersed in 25 mL of a 70% ethanolic solution at 10°C and stirred at 100 rpm. For measurement purposes, 2 mL of release medium were withdrawn at predetermined times. Its absorbance was determined at 271 nm using a UV-1800 UV-Vis spectrophotometer (Shimadzu). This aliquot was returned after reading, and the system was kept under stirring until the next reading [23].

Food protection test. The antioxidant activity of the films with hydroalcoholic extracts was tested on halved Hass avocados. The cut face was covered with simple films and those incorporated with hydroalcoholic extract. The research involved an additional Hass avocado test without coating, which was marked as control sample C. The tests were carried out at 8°C and 50–60% relative humidity on storage day 21.

RESULTS AND DISCUSSION

Total phenolic content and antioxidant activity of extracts. A 10-g sample of *Macrocystis pyrifera* L. yielded 6.86% in the extraction of the hydroalcoholic extract. Its concentration was 10% w/v, the TFC was 74.2 mg GAE 100 g⁻¹, and the percentage inhibition was 61.0%.

After that, 3 and 6% solutions were prepared from diluted stock solution. They were presented as a total polyphenol content of 25.4 and 48.5 mg GAE 100 g⁻¹, with inhibition percentages of 22.2 and 41.2%, respectively. The obtained results were consistent with available scientific publications on *M. pyrifera*. Table 1 shows the total phenolic content values for each solution.

a   b   c
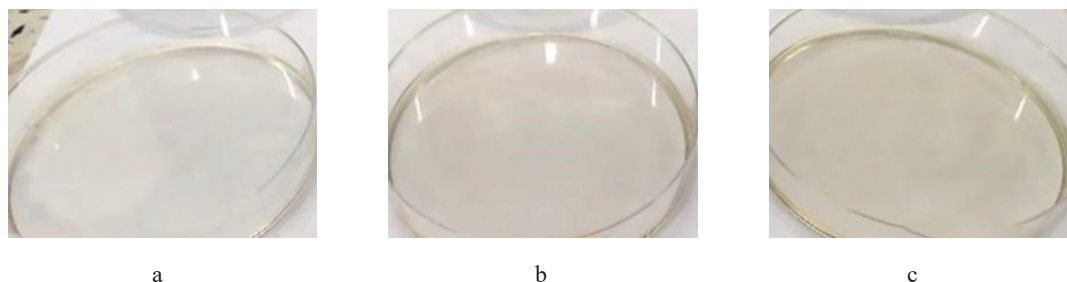
Figure 1 Films obtained from sodium alginate: (a) base film (no extract); (b) film with 3% hydroalcoholic *Macrocystis pyrifera* extract; and (c) film with 6% extract
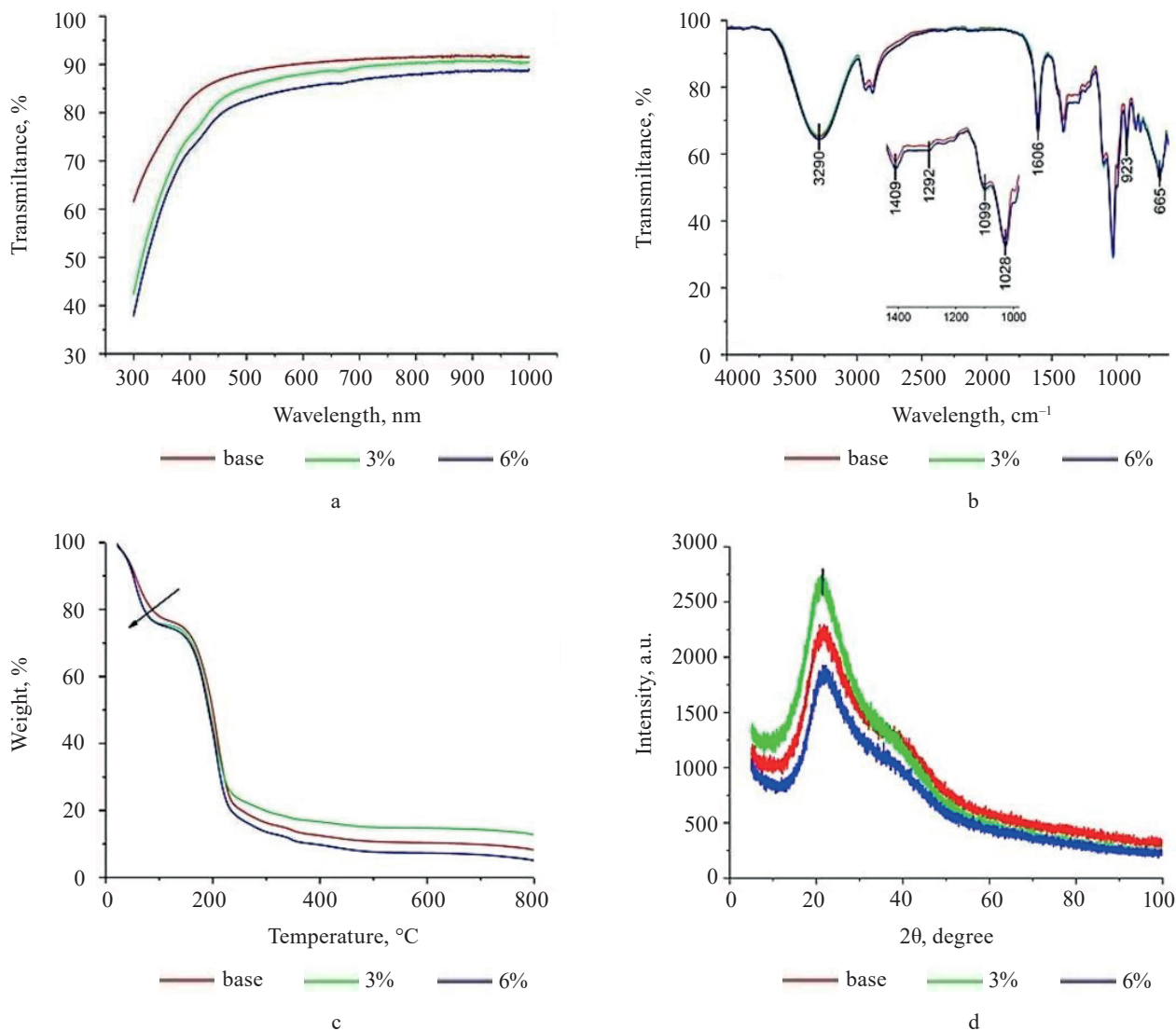
Figure 2 Light transmittance (a), FTIR spectrum (b), TG curves (c), and XRD diffractograms (d) of films from sodium alginate (base) and sodium alginate with 3 and 6% of *Macrocystis pyrifera* extract

Table 2 Transmittance and opacity values of films in the visible spectrum

Film	Thickness, mm	T_{600}, %[a]	Opacity, a.u. (nm/mm)
Base (no extract)	0.185	90.2059	0.24
With 3% *Macrocystis pyrifera* extract	0.173	87.9631	0.32
With 6% *Macrocystis pyrifera* extract	0.178	85.2594	0.39

[a] T_{600} % is the transmittance percent of each film at 600 nm

Sodium alginate films. We prepared three alginate films, namely the base film, which contained no hydro-alcoholic extract, and films contained 3 and 6% of hydroalcoholic extract. Figure 1 depicts the obtained films: the hue darkened as the concentration of the hydroalcoholic extract increased.

Optical properties of films. Average thickness and UV-Vis spectrum described the opacity of the films (Fig. 2a). The obtained transmittance percentage was $\geq$ 80% in the region of 500–800 nm. The transmittance decreased as the hydroalcoholic extract concentration increased because it had a photoprotective effect [24]. The opacity also increased, which means that the extracts were not homogeneously distributed in the polymeric matrix of the films.

Table 2 shows the transmittance value of the films at 600 nm (visible light), as well as their corresponding opacity. The transmittance percentage of the base film was 90.21%. As the concentration of the extract increased, the value fell down to 87.96 and 85.26% in the films with 3 and 6% of the extract, respectively. The opacity was calculated at a wavelength of 600 nm. It demonstrated a slight increase as the concentration of the *M. pyrifera* extract increased.

Table 3 Mass loss values: thermogravimetric analysis of films obtained from sodium alginate with/without *Macrocystis pyrifera* extract

Film	Weight, mg	Thermal event	ΔT, °C	Mass loss, %
Base (no extract)	5.176	Dehydration	25.0–119.8	22.8
		Film degradation	119.8–320.8	61.1
		Polymer degradation	320.8–672.5	5.38
		Carbonization	672.5–800.0	5.14
With 3% *Macrocystis pyrifera* extract	5.142	Dehydration	25.0–109.7	23.9
		Film degradation	109.7–325.5	57.0
		Polymer degradation	325.5–638.2	4.00
		Carbonization	638.2–800.0	7.87
With 6% *Macrocystis pyrifera* extract	5.105	Dehydration	25.0–113.6	24.8
		Film degradation	113.6–314.1	61.9
		Polymer degradation	314.1–617.3	5.68
		Carbonization	617.3–800.0	9.86
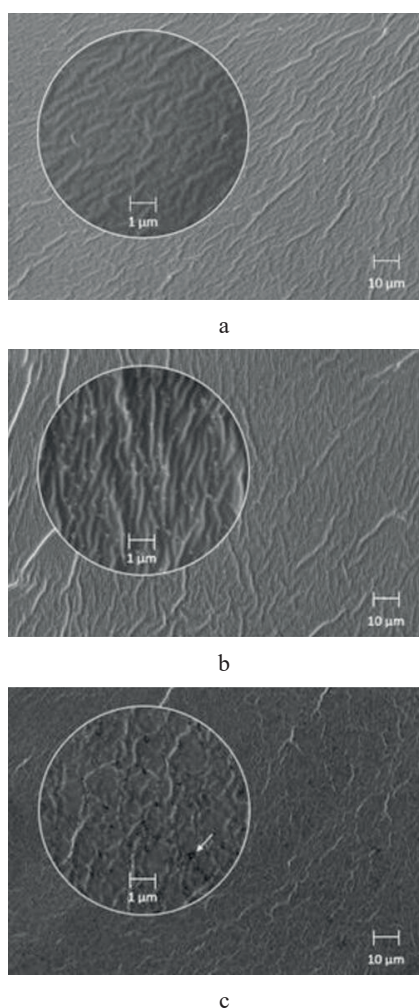
Figure 3 Scanning electron microscopy images of films: (a) base film; (b) film with 3% extract; and (c) film with 6% extract

FTIR of the films. Figure 2b illustrates the FTIR spectrum of the films under study. The increase in the concentration of the extracts intensified the bands corresponding to the symmetric stretching COO⁻ at 1409 cm^{-1}, torsional vibrations and swinging of –CH$_2$ at 1350–1150 cm^{-1}, C-O stretching of the pyranose ring at 1099 cm^{-1}, and C-O stretching at 1028 cm^{-1} of sodium alginate [25–27]. The obtained results revealed an interaction between the polar groups of the polymeric matrix and the polyphenolic compounds of the extract.

Thermogravimetry. Figure 2c presents the thermogravimetric curves of the films with mass losses that were assigned to the following steps: dehydration, film degradation, polymer degradation, and carbonization [28]. As the extracts became more concentrated, the mass loss in the films increased, especially in the film with 6% of the extract. However, if the concentration of the extract was lower, the mass loss decreased during this step, and a better extract-film interaction was assumed. Table 3 summarizes the thermal events, mass loss, and respective temperature intervals

X-ray diffraction analysis. The X-ray diffraction diffractogram in Fig. 2d demonstrates a broad peak between 20 and 30°. It presents the diffraction pattern of the amorphous structure of the sodium alginate film plasticized with glycerol and PEG 400 (base film). The crystallinity percentage of the base film was 39.3%. However, it reached 39.1% when it was incorporated with 6% of the extract. The low concentration of the extract brought up the crystallinity to 43.1% in the film with 3% of the extract. Therefore, the microstructure of the incorporated film was more homogeneous when the concentration of the extract was lower.

Scanning electron microscopy analysis. The scanning electron microscopy images (Figs. 3a, 3b, and 3c) showed a rough and homogeneous surface (Fig. 3a) with clusters on the surface, which increased the concentration of the *M. pyrifera* extract (Figs. 3b and 3c). The obtained result shows how the secondary metabolites migrated towards the avocado surface.

Kinetic behavior of hydroalcoholic extract release. Figure 4 shows the release curve of the extract at 271 nm for 300 min of testing. Figure 5 indicates the profile of the film with 3 and 6% extract according to the Higuchi model. Figure 6 shows the profile according to
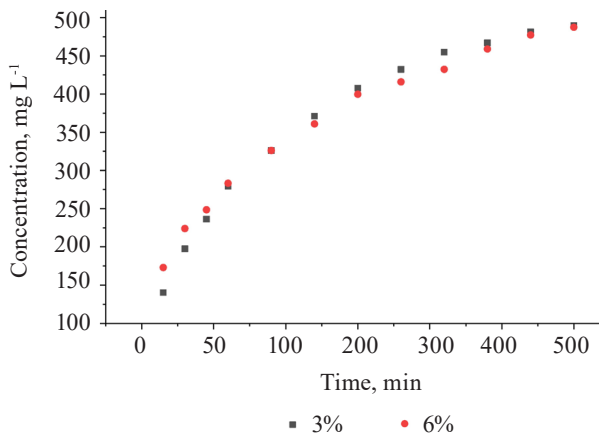
Figure 4 Release profile of *Macrocystis pyrifera* extract in alginate films with 3 and 6% hydroalcoholic *Macrocystis pyrifera* extracts
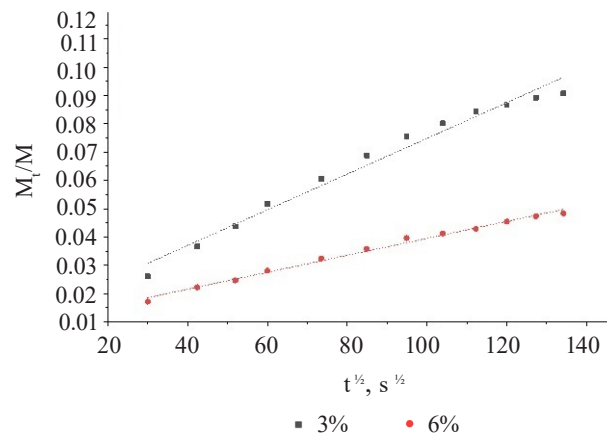
Figure 5 Release profile according to the Higuchi model.
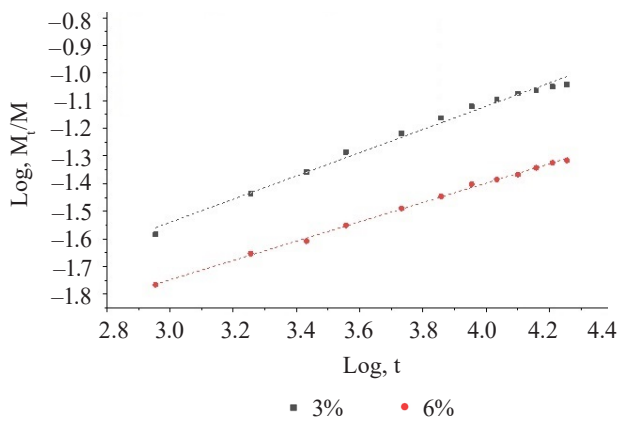
**Figure 6** Release profile according to the Korsmeyer and Peppas model.

Table 4 Kinetic parameters of films from sodium alginate with *Macrocystis pyrifera* extracts according to Higuchi and Korsmeyer-Peppas

Film	Higuchi		Korsmeyer-Peppas	
	K_H	R^2	n	R^2
3% extract	6.31×10^{-4}	0.9764	0.42	0.9894
6% extract	2.99×10^{-4}	0.9918	0.35	0.9982

to the Korsmeyer and Peppas model. In both cases, the film with the 3% extract had higher constants R^2 and n. However, the film with the 6% extract could continue to release. The release percentage was not complete because the extract contained polyphenolic compounds: their hydroxyl groups can interact with related groups of alginate or plasticizer [23].

Table 4 shows kinetic parameters K and n calculated according to Eqs. (3) and (4). As $n \leq 0.5$, the swelling and porosity provided a partial diffusion mechanism [29].

Food protection test. In Fig. 7, the endocarp of the control sample (uncoated avocado) is brown around the stone, and so is the sample coated with the base film
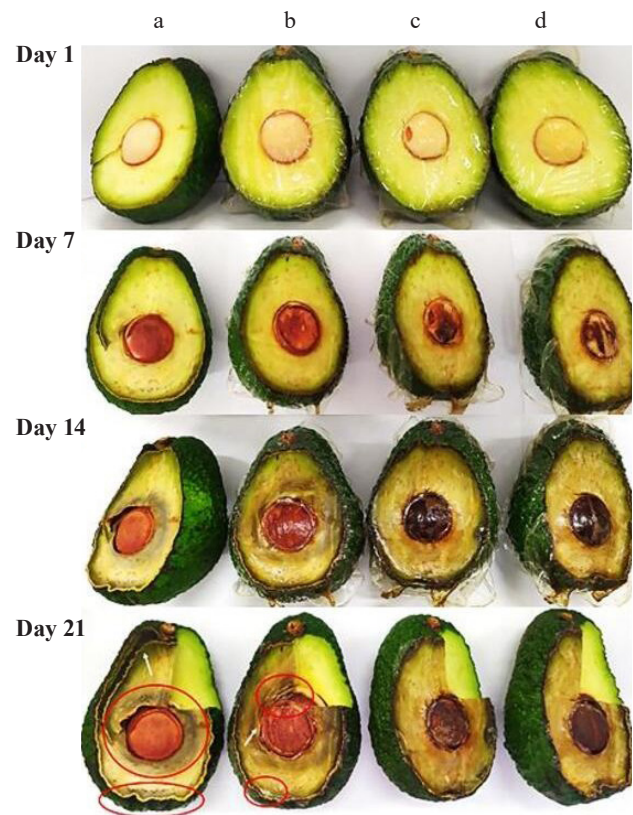
Figure 7 Hass avocado halves on days 1, 7 and 14 of storage. Epicarp, mesocarp, and endocarp of Hass avocado on day 21. (a) Uncoated (control); (b) coated with the base film (no extract); (c) coated with the film from sodium alginate with the 3% *Macrocystis pyrifera* hydroalcoholic extract; and (d) coated with the film from sodium alginate with the 6% extract

(no *M. pyrifera* extract). However, as the concentration of the hydroalcoholic extract increased, the browning intensity around the stone decreased. As a result, the browning in the sample covered with the film with the 6% extract was less intense in color, compared to the avocado covered with the film with the 3% extract. This result proves that the extract migrated from the film onto the fruit surface.

On day 21, none of the samples showed any evidence of browning. Therefore, the interior of the fruit remained intact under the experimental conditions of 8°C and 50–60% relative humidity. However, the epicarp in the control sample and the avocado coated with the base film had a little mold caused by humidity, which was absent in the samples coated with the films with the *M. pyrifera* extracts.

CONCLUSION

The hydroalcoholic extracts interacted with the polymeric matrix of sodium alginate. The increase in their concentration affected the surface and the microstructure of the films, resulting in a greater mass loss during degradation, a more intense opacity, and a lower crystallinity percentage. However, when the concentration was lower, it facilitated the distribution within the polymeric matrix. Alginate films proved to be good vehicles for the administration and release of *Macrocystis pyrifera* extracts. If used as fruit coating, this film can reduce browning.

CONTRIBUTION

The authors were equally involved in the written and experimental part of the manuscript and are equally responsible for plagiarism.

CONFLICT OF INTEREST

The authors declare no conflict of interests regarding the publication of this article.

REFERENCES

1. Bahl S, Dolma J, Singh JJ, Sehgal S. Biodegradation of plastics: A state of the art review. Materials Today: Proceedings. 2020;39:31–34. https://doi.org/10.1016/j.matpr.2020.06.096

2. Shlush E, Davidovich-Pinhas M. Bioplastics for food packaging. Trends in Food Science and Technology. 2022;125:66–80. https://doi.org/10.1016/j.tifs.2022.04.026

3. Teixeira-Costa BE, Andrade CT. Natural polymers used in edible food packaging – History, function and application trends as a sustainable alternative to synthetic plastic. Polysaccharides. 2022;3(1):32–58. https://doi.org/10.3390/polysaccharides3010002

4. Ibrahim NI, Shahar FS, Hameed Sultan MT, Shah AU, Azrie Safri SN, Mat Yazik MH. Overview of bioplastics introduction an its applications in product packaging. Coatings. 2021;11(11). https://doi.org/10.3390/coatings11111423

5. Rosa GP, Tavares WR, Sousa PMC, Pagès AK, Seca AML, Pinto DCGA. Seaweed secondary metabolites with beneficial health effects: An overview of successes in in vivo studies and clinical trials. Marine Drugs. 2020;18(1). https://doi.org/10.3390/md18010008

6. Tenorio-Rodríguez PA, Esquivel-Solis H, Murillo-Álvarez JI, Ascencio F, Campa-Córdova ÁI, Angulo C. Biosprospecting potential of kelp (Laminariales, Phaeophyceae) from Baja California Peninsula: Phenolic content, antioxidant properties, anti-inflammatory, and cell viability. Journal of Applied Phycology. 2019;31(5):3115–3129. https://doi.org/10.1007/s10811-019-01781-1

7. Ford L, Stratakos AC, Theodoridou K, Dick JTA, Sheldrake GN, Linton M, *et al.* Polyphenols from Brown Seaweeds as a potential antimicrobial agent in animal feeds. ACS Omega. 2020;5(16):9093–9103. https://doi.org/10.1021/acsomega.9b03687

8. Murúa P, Edrada-Ebel R, Muñoz L, Soldatou S, Legrave N, Müller DG, *et al.* Morphological, genotypic and metabolomic signatures confirm interfamilial hybridization between the ubiquitous kelps *Macrocystis* (Arthrothamnaceae) and *Lessonia* (Lessoniaceae). Scientific Reports. 2020;10(1). https://doi.org/10.1038/s41598-020-65137-3

9. Tapia-Martínez J, Cano-Europa E, Casas-Valdez M, Blas-Valdivia V, Franco-Colin M. Toxicological and therapeutic evaluation of the algae *Macrocystis pyrifera* (Phaeophyceae) in rodents. Revista de Biologia Marina y Oceanografia. 2020;55(2):119–127. https://doi.org/10.22370/rbmo.2020.55.2.2497

10. Rodríguez JE, Castro A. Evaluation of polyphenol content and antioxidant activity of the hydroalcoholic extract of *Eisenia cokeri* m.a. howe. Ciencia e Investigación. 2018;21(1):11–17. (In Spanish).

11. Beratto-Ramos A, Castillo-Felices RP, Troncoso-León NA, Agurto-Muñoz A, Agurto-Muñoz C. Selection criteria for high-value biomass: Seasonal and morphological variation of polyphenolic content and antioxidant capacity in two brown macroalgae. Journal of Applied Phycology. 2019;31(1):653–664. https://doi.org/10.1007/s10811-018-1528-9

12. Ore YB, Pichilingue ERL, Valderrama Negron AS. Extraction and characterization of sodium alginate from the macroalgae *Macrocystis pyrifera*. Revista de la Sociedad Química del Perú. 2020;86(3):276–287. (In Spanish). https://doi.org/10.37761/rsqp.v86i3.300

13. Layek B, Mandal S. Natural polysaccharides for controlled delivery of oral therapeutics: A recent update. Carbohydrate Polymers. 2020;230. https://doi.org/10.1016/j.carbpol.2019.115617

14. Santos LG, Silva GFA, Gomes BM, Martins VG. A novel sodium alginate active films functionalized with purple onion peel extract (*Allium cepa*). Biocatalysis and Agricultural Biotechnology. 2021;35. https://doi.org/10.1016/j.bcab.2021.102096

15. Azucena Castro-Yobal M, Contreras-Oliva A, Saucedo-Rivalcoba V, Rivera-Armenta JL, Hernández-Ramírez G, Salinas-Ruiz J, *et al.* Evaluation of physicochemical properties of film-based alginate for food packing applications. E-Polymers. 2021;21(1):82–95. https://doi.org/10.1515/epoly-2021-0011

16. Silva J, Vanat P, Marques-da-Silva D, Rodrigues JR, Lagoa R. Metal alginates for polyphenol delivery systems: Studies on crosslinking ions and easy-to-use patches for release of protective flavonoids in skin. Bioactive Materials. 2020;5(3):447–457. https://doi.org/10.1016/j.bioactmat.2020.03.012

17. Solano-Doblado LGa, Alamilla-Beltrán L, Jiménez-Martínez C. Functionalized edible films and coatings. TIP Revista Especializada en Ciencias Químico-Biológicas. 2018;21(2):30–42. (In Spanish). https://doi.org/10.22201/fesz.23958723e.2018.0.153

18. Higuchi T. Mechanism of sustained action medication. Theoretical analysis of the rate of release of solid drugs dispersed in solid matrices. Journal of Pharmaceutical Sciences. 1963;52(12):1145–1149. https://doi.org/10.1002/jps.2600521210

19. Korsmeyer RW, Gurny R, Doelker E, Buri P, Peppas NA. Mechanisms of solute release from porous hydrophilic polymers. International Journal of Pharmaceutics. 1983;15(1):25–35. https://doi.org/10.1016/0378-5173(83)90064-9

20. Vilcanqui Y, Mamani-Apaza LO, Flores M, Ortiz-Viedma J, Romero N, Mariotti-Celis MS, *et al.* Chemical characterization of brown and red seaweed from Southern Peru, a sustainable source of bioactive and nutraceutical compounds. Agronomy. 2021;11(8). https://doi.org/10.3390/agronomy11081669

21. Liu X, Yuan W, Zhao R. Extraction of antioxidants from brown algae *Ascophyllum nodosum* using a binary solvent extraction system. ACS Food Science and Technology. 2021;1(6):1041–1049. https://doi.org/10.1021/acsfoodscitech.1c00053

22. Cui R, Zhu B, Yan J, Qin Y, Yuan M, Cheng G, Yuan M. Development of a sodium alginate-based active package with controlled release of cinnamaldehyde loaded on halloysite nanotubes. Foods. 2021;10(6). https://doi.org/10.3390/foods10061150

23. Carlos-Salazar MJ, Valderrama-Negrón AC. Release of anthocyanins from chitosan films cross-linked with sodium tripolyphosphate. Revista de la Sociedad Química del Perú. 2017;83(1):115–125. https://doi.org/10.37761/rsqp.v83i1.108

24. Castro AJ, Carhuapoma M, Ramos NJ, Juárez JR, Felix LM, Jáuregui JF, *et al.* Photoprotective effect of *Macrocystis pyrifera* compared to sunscreens in prevention of skin lesions. Ciencia e Investigación. 2015;18(2):95-98. (In Spanish). https://doi.org/10.15381/ci.v18i2.13617

25. Ye Y, Zhang X, Deng X, Hao L, Wang W. Modification of alginate hydrogel films for delivering hydrophobic kaempferol. Journal of Nanomaterials. 2019;2019. https://doi.org/10.1155/2019/9170732

26. Fabra MJ, Falcó I, Randazzo W, Sánchez G, López-Rubio A. Antiviral and antioxidant properties of active alginate edible films containing phenolic extracts. Food Hydrocolloids. 2018;81:96–103. https://doi.org/10.1016/j.foodhyd.2018.02.026

27. Mutlu B, Farhan M, Kucuk I. T-Shaped microfluidic junction processing of porous alginate-based films and their characteristics. Polymers. 2019;11(9). https://doi.org/10.3390/polym11091386

28. Zia T, Usman M, Sabir A, Shafiq M, Khan R. Development of inter-polymeric complex of anionic polysaccharides, alginate/k-carrageenan bio-platform for burn dressing. International Journal of Biological Macromolecules. 2020;157:83–95. https://doi.org/10.1016/j.ijbiomac.2020.04.157

29. Aragón Fernández J, González Santos R, Fuentes Esteves G. Study in vitro of delivery drug from a compound biomaterial. Revista CENIC. Ciencias Químicas. 2010;41:1–8. (In Spanish).

ORCID IDs
Judith Ramos https://orcid.org/0000-0003-2434-9197
Nelson Adrián Villacrés https://orcid.org/0000-0001-9499-3792
Éder Tadeu Gomes Cavalheiro https://orcid.org/0000-0002-5186-3039
Hugo A. Alarcón https://orcid.org/0000-0002-9533-2133
Ana C. Valderrama https://orcid.org/0000-0001-7741-3207